ACS APPLIED MATERIALS & INTERFACES

Research Article

www.acsami.org

Highly Ordered, Hierarchically Porous TiO_2 Films via Combination of Two Self-Assembling Templates

Wonho Kim, Su Yeon Choi, Young Moo Jeon, Seung-kyu Lee, and Seung Hyun Kim*

Department of Applied Organic Materials Engineering, Inha University, Incheon 402-751, Republic of Korea

Supporting Information

ABSTRACT: Hierarchically mesoporous TiO_2 films with a high degree of order and connectivity on the sub-100-nm scale are successfully fabricated by the dual-templating methods sequentially applied. In this approach, the self-assembly of block copolymers combined with sol–gel reaction is first used to generate highly ordered mesoporous films by optimizing their self-assembling behavior. At the next step, 50-nm PS nanoparticles are deposited on the mesoporous films generated in the previous step to produce the colloidal crystals, and their inverse structure with a high degree of order, otherwise, would not form the colloidal crystals but generate a colloidal glassy phase with poor order. In addition to the exceptionally high degree of order, mesoporous films exhibit a high porosity that spans from the top surface to the bottom surface throughout the entire film without clogging. Especially wide pores at the top layer enable functional materials of large size to access the inside the films with small pores, maximizing their performance. As a proof of concept, photocatalytic effects are examined for the mesoporous films with different structures. In terms of the template pattern, the line pattern and bowl structure are also shown to guide the self-assembly of colloidal particles when their characteristic size matches with the particle diameter, in addition to the hexagonal packing.

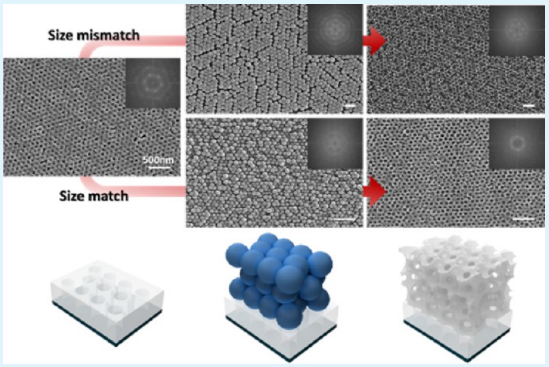

KEYWORDS: *self-assembly, block co-polymer, colloidal particles, templating, hierarchical pores*

INTRODUCTION

Well-ordered mesoporous and microporous titania (TiO_2) films have attracted much attention, because of a wide range of potential applications, including photonics, optoelectronics, photovoltaic cells, sensors, data storage, nanolithography, and catalysts that could utilize their remarkable electronic and optical properties.[1−9] To realize such potentials in real applications, however, there should be continuous innovations in methodology to produce and manipulate well-controlled, much-complicated structure on the nanometer scale. In the case of porous titania films, controlling their morphology is key for the best performance, because many of these applications require a large interfacial area, controlled pore orientation and size, open-cellular interconnectivity, and adjustable functionalities. Here, we present fabrication results of better-controlled, more-complicated TiO_2 porous films through the combination of two templating methods, which is conceptually simple yet can be very effective to fabricate hierarchically porous films on a sub-100-nm scale.

Many strategies have been developed for generation of porous titania films over two decades. Among them, the sol–gel technique, in combination with a templating method, has been widely used, because of its simple processing and versatility in the formation of a porous structure with various patterns and size.[10−14] The template used in this process is removed after the formation of the structure so that it leaves pores in the remaining materials and consequently determines the resulting pore structure. Various types of templates have been investigated to explore their structure-directing ability in pore formation, and since the discovery of mesoporous silica, which was first synthesized by Mobil's researchers, self-assembling soft materials including supramolecular surfactants, block co-polymers (BCPs), and colloidal particles have been successfully used for generation of pores with the size ranging from a few nanometers to hundreds of micrometers.[15−19] The choice of template as a structure-directing agent is very decisive in determining the type and quality of porous structure, and the choice should be made carefully, considering its application. For example, low-molecular-weight surfactants have intensively been used as a template in the early days, but the resulting pores were too small to be accessed in many cases. Consequently, the structure-directing agents capable of producing pores with larger size, such as BCPs or colloidal particles, have attracted more attention for the utilization of pores.

BCPs composed of chemically different polymers covalently joined at one end self-assemble into ordered periodic structures on the nanometer scale. The structure and size of self-

Received: April 10, 2014
Accepted: June 24, 2014
Published: June 24, 2014

Scheme 1. Fabrication Procedure of Hierarchically Mesoporous TiO_2 Films by Use of the Dual-Templating Method Based on the Self-Assembly of Block Co-polymers (BCPs) and Colloidal Particles: (a) Self-Assembly of BCP Containing Titanium Precursors, (b) Calcination for Mesoporous TiO_2 Template, (c) Self-Assembly of Colloidal Particles on the Template, (d) Infiltration of Titanium Precursors into Colloidal Crystal, and (e) Calcination for Hierarchically Mesoporous TiO_2 Film

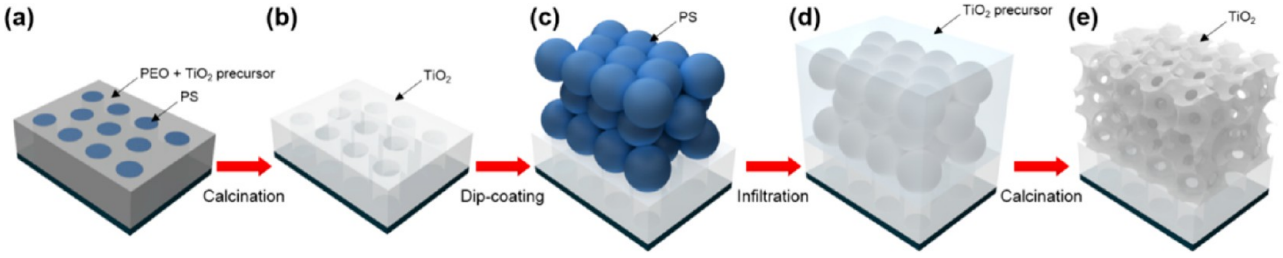

assembled BCPs can be tuned by their molecular weight and block composition, which makes these materials particularly attractive as a template for the synthesis of nanostructured materials. In terms of mesoporous TiO_2 films, the titanium precursors are selectively loaded into one microdomain through specific interactions with specific block components to form organic/inorganic hybrids. Subsequent hydrolysis/condensation of precursors and removal of BCPs via thermolysis produce well-defined mesoporous TiO_2 films, the structure of which simply follows the one generated by BCP self-assembly.[20−26] Therefore, in this process, BCPs play a key role as a structure-directing agent and a sacrificial template in the formation of porous titania films on the tens of nanometers scale. However, in most cases, BCP self-assembly in the presence of inorganic precursors was extremely difficult to control, because of the interaction with the precursors that were highly reactive, and so the porous structure deviated from the ideal BCP nanostructure and very often suffered from the lack of a well-defined, long-range order in their applications.

Colloidal particles are another class of self-assembling materials that, as a template, can guide and direct the resulting porous structure in the submicrometer range. Generally, they self-assemble to form colloidal crystals with a highly ordered crystalline structure. In that case, the infiltration of the interstitial space between the particles with an inorganic sol, and subsequent hydrolysis/condensation reaction, together with the removal of colloidal particles, generate a porous network structure. The resulting pore size can be easily controlled by changing the size of colloidal particles, which imparts controls over the detailed structure of porous materials. In addition to the facile and inexpensive fabrication of periodic nanostructures over a large area, the high porosity generated in this process makes this approach very attractive in many applications that require it.[25,27−30] In this approach, controlling the quality of colloidal crystals generated via self-assembly is key, because it critically determines the porosity and mechanical integrity of the pore structure. Colloidal particles with the size ranging from hundreds of nanometers to micrometers have been demonstrated to be able to produce high-quality colloidal crystal with a well-ordered structure that could be readily used as a template for an inverse opal structure. However, as the particle size for smaller pore structure decreases, it becomes extremely difficult to generate a highly ordered crystal array of nanoparticles, and a colloidal glassy phase, instead of colloidal crystal, forms because of enhanced Brownian motion, poor monodispersity, and smaller interacting forces between particles, which limits their full utilization in applications.

In this work, two self-assembling materials, BCPs and colloidal particles, are applied together as structure-directing templates to produce porous TiO_2 films. Such a combination approach for porous TiO_2 films is not new, but has already been reported in the literature.[31−33] In that approach, the self-assembly of BCP has been used to generate a porous bottom layer, upon which the second self-assembling colloidal particles have been deposited to produce double-porous layers with different length scales. Furthermore, it has been demonstrated that such double-porous films can provide efficient platforms for improving photon-to-electron conversion efficiency and the light harvesting ability. The approach employed in the present work is very similar, where the sequential use of two self-assembling materials is adopted to direct the structure and generate the pores with different sizes. However, our focus is placed on controlling the self-assembly of colloidal particles with sub-100-nm size for highly ordered pore structure; otherwise, it would never form highly ordered colloidal crystals nor their well-defined inverse porous structure. An essential prerequisite to establish such a goal is to generate a highly ordered template over a large area that is size-matched with colloidal particles. In our work, through fine-tuning of the BCP self-assembly and sol−gel chemistry, a highly ordered porous film is produced and used as a template, and, consequently, each colloidal particle of very small size sits on the pores of the bottom layer to form colloidal crystals with a high degree of order. Scheme 1 schematically illustrates the overall procedure for the fabrication of mesoporous TiO_2 films followed in our route. As a result, the self-assembly of colloidal particles will be directed by the porous film structure underneath them, and then the infiltration and calcination of titania sol−gel precursor into colloidal crystals produce hierarchically porous films with two different structures and length scales but with pores connected from the top to the bottom in the end.

EXPERIMENTAL SECTION

Materials. Two polystyrene-*block*-poly(ethylene oxide) (PS-*b*-PEO) BCPs with different molecular weights, purchased from Polymer Source, Inc., were used in this work. One has a molecular weight of 30 000 g mol^{-1} with 77 wt % polystyrene (PS), and the other has a molecular weight of 43 000 g mol^{-1} with 74% PS, thus both forming PEO cylinders in the PS matrix in the bulk. Suspensions of PS colloidal particles with different sizes of 200 nm (standard deviation (Std Dev) = 3.4 nm, coefficient of variation (CV) = 1.7%), 100 nm (Std Dev = 4.5 nm, CV = 4.6%), and 50 nm (Std Dev = 7.2 nm, CV = 15.7%) diameter were purchased from Duke Scientific. Titanium isopropoxide (TTIP), which was used as an inorganic

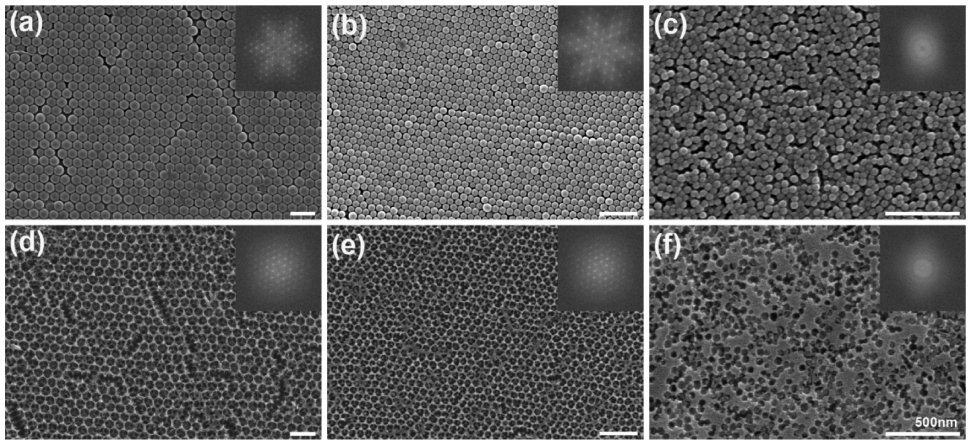

Figure 1. SEM images of (a, b, c) colloidal crystals and (d, e, f) their inverse opals fabricated on flat silicon substrate by PS colloidal particles of different diameters of (a, d) 200 nm, (b, e) 100 nm, and (c, f) 50 nm. The insets in each figure correspond to the FFT results of SEM images.

precursor, was purchased from Acros Organics. All solvents for BCP and titanium precursor solutions including 1,4-dioxane, toluene, HCl, and isopropyl alcohol (IPA) were used as received without further purification.

Template Preparation Based on BCP. The first mesoporous TiO_2 films, which would be used as a template at the next step, were prepared by the combination of BCP self-assembly and sol−gel reaction. First, BCP and the precursor solutions are prepared separately: PS-*b*-PEO BCPs were dissolved in 1,4-dioxane while, as a titanium precursor, 0.297 mL of TTIP and 0.110 mL of HCl were added into 2 mL of IPA and then stirred for 2 h.[22] BCP solution and titanium precursor were mixed at a predetermined volume ratio and stirred for 1 h before use. The films were deposited by spin-coating onto a Si wafer substrate under controlled relative humidity (RH) and were calcined at 500 °C to remove PS-*b*-PEO BCP and produce mesoporous titania film. (See step (b) in Scheme 1.) The film thickness was controlled by solution concentration and set to be ∼100 nm after calcination. Before spin-coating, the silicon wafer was cleaned in piranha solution (70/30, v/v, H_2SO_4/H_2O_2) at 90 °C for 30 min and thoroughly rinsed with deionized (DI) water, and then blown dry with N_2 gas.

Template Preparation Based on Colloidal Particles. For controlling the self-assembly of PS colloidal particles, self-assembled colloidal crystals 200, 100, and 50 nm in diameter were fabricated on the titania template that had been generated at the previous step. (See step (c) in Scheme 1.) The fabrication of colloidal crystals was carried out via a solvent−evaporation-induced dip-drawing method at 50 °C. The concentration of colloidal particles in aqueous solution was controlled to produce a constant number of layers in all cases, and the duration time and the withdrawl rate of the substrate in solution were kept constant throughout the experiments. The solution temperature and withdrawl rate are important parameters related to the evaporation rate and film formation, but their detailed effects are outisde of the scope of this study and are not pursued here. For comparison, colloidal crystals were produced on bare Si wafers without prepatterns under the same conditions. Other porous films were prepared through the infiltration of TiO_2 precursors into colloidal crystal and subsequent calcination at 500 °C in air. (See steps (d) and (e) in Scheme 1.) The precursor used here was the same as in the previous section, and its amount of infiltration was controlled, to avoid the formation of layers over the colloidal crystals.

Characterization and Measurements. The structures of organic/inorganic composite films, colloidal crystals, and mesoporous TiO_2 films were characterized by using tapping-mode atomic force microscopy (AFM), field-emission scanning electron microscopy (FE-SEM), and grazing-incidence small-angle X-ray scattering (GISAXS). The tapping-mode AFM equipment used for characterization of the surface morphology was MultiMode V Scanning Probe Microscope (Digital Instruments/Veeco). AFM images were recorded by aluminum-coated silicon cantilevers with a resonance frequency of 285 kHz and a spring constant of 42 N/m. FE-SEM was performed on a Hitachi Model S-4300SE SEM microscope operated at 15.0 kV. GISAXS measurements were performed on the 4C2 beamline at Pohang Accelerator Laboratory (PAL) in Korea to obtain the structural information inside the mesoporous films. The wavelength and sample-to-detector distance was 1.3807 Å and 2.241 m, and the scattered signal was recorded with a two-dimensional (2D) CCD camera with 1042 × 1042 pixels of a size of 115.2 μm × 115.2 μm. The scattering patterns were taken above the critical angle of mesoporous films to examine the structures inside the film. For characterization of photocatalytic activity, Methylene Blue (MB) solution was prepared by dissolving 5 ppm of MB powder in distilled water. Mesoporous TiO_2 films were placed at the bottom of the vials filled with MB solution. Each vial containing TiO_2 catalysts was exposed to ultraviolet (UV) light with a wavelength of 254 nm. The absorbance of MB solution irradiated by UV light was measured every 30 min by UV-vis spectrometer (Shimadzu, Model UV-1601PC).

RESULTS AND DISCUSSION

Before using the templates for guidance of colloidal self-assembly, colloidal crystals with different diameters were first grown on a nonpatterned substrate for comparison. Colloidal crystals can be fabricated by several methods such as gravity sedimentation, vertical deposition, electrophoresis, solvent evaporation, membrane filtration, and the Langmuir−Blodgett method.[13,34−39] In this work, the vertical deposition technique, using the dip-drawing method, was applied to fabricate colloidal crystals, since it could easily produce the crystal structure with a well-define shaped and enhanced lateral order. The results are shown in Figure 1 for PS colloidal particles with different sizes.

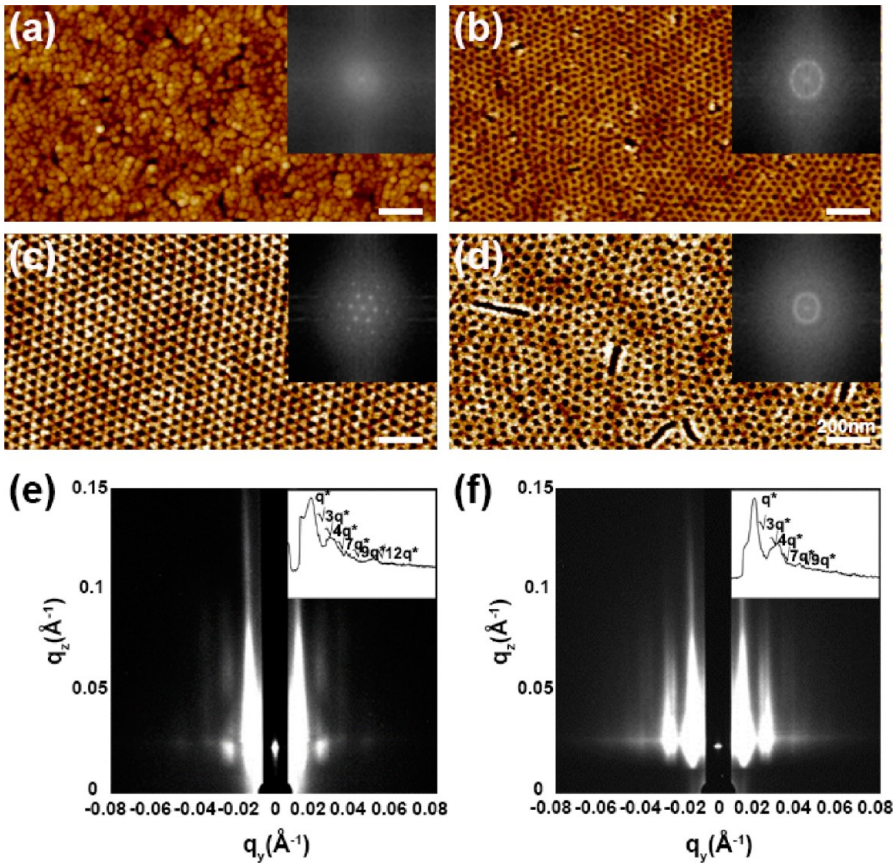

Figure 2. AFM images of mesoporous TiO_2 films produced by combination of sol−gel reaction with BCP self-assembly at different concentrations of BCP/TTIP of (a) 100/50, (b) 100/100, and (c) 100/180 at a relative humidity (RH) = 70%, and (d) 100/180 at RH = 40%. GISAXS patterns of TiO_2 films described in panel c before calcination (panel e) and after calcination (panel f). The insets in panels a, b, c, and d show the FFT results of the AFM images.

As expected, 200- and 100-nm PS nanoparticles in Figures 1a and 1b can readily produce highly ordered colloidal crystals of hexagonally close-packed structure without any assistance; on the other hand, particles as small as 50 nm in size exhibit poor order in the array of colloidal particles, forming the colloidal glass instead of colloidal crystal, as seen in Figure 1c. The fast Fourier transform (FFT) results presented in the insets directly reveal the degree of order of colloidal crystals fabricated on the flat substrate. Self-assembled structure of 50-nm PS colloidal particles is mainly due to the polydispersity in their size distribution, because all procedures and conditions affecting the quality of colloidal crystal are the same for all PS particles, except their size and size distribution. As described in the Experimental Section, 50-nm PS particles have a wider size distribution than other PS particles. Even with the same polydispersity, it can be expected that its effects are more prominent in colloidal particles with smaller size. The same results have been found in colloidal crystals fabricated by different approaches such as drop-casting and sedimentation. (See Figure S1 in the Supporting Information.) Figures 1d, 1e, and 1f correspond to the inverse structures that are generated through infiltration of titanium precursors into the colloidal crystals and then calcination for the removal of the PS particles. They exactly reflect the order quality of original templates, exhibiting highly ordered TiO_2 inverse structure in the case of 200- and 100-nm PS particles (Figures 1d and 1e) but poor order in TiO_2 inverse structure from 50-nm PS colloidal arrays (Figure 1f). Consequently, the results in Figure 1 indicate that the self-assembly alone is not enough to generate well-defined colloidal crystals in the case of 50-nm-size colloidal particles, suggesting that an additional external field should be required for guidance of self-assembly to achieve a high degree of order in colloidal crystals.

In order to generate the colloidal crystals and improve their stacking order for colloidal particles with 50 nm size on the sub-100-nm scale, in this work, the template-based guidance is employed to direct the colloidal self-assembly. The most important requirements of the template for guidance of the self-assembly are the size match between the template pattern and colloidal particles and well-controlled pattern of template to achieve highly ordered colloidal crystals. In this respect, BCP can be an ideal template, since the shape and size of its patterns can be adjusted by controlling the molecular parameters including the molecular weight and block composition to match the size of colloidal particles and their self-assembled patterns. As a template for colloidal self-assembly, in our approach, BCP self-assembly is combined with sol−gel reaction to produce TiO_2 mesoporous films. Then, the pores in the mesoporous films, whose pattern and size will be determined by BCP self-assembly, will ultimately guide the self-assembly of colloidal particles. This template fabrication process is basically simple and can spontaneously proceed without any special tools or assistance. However, several parameters such as the composition of precursor solution, the choice of solvent, the relative amount of BCP and sol−gel precursor, and processing conditions can affect the quality of the final mesoporous

structure; therefore, such variables should be optimized for BCP self-assembling process combined with sol−gel reaction to produce highly ordered mesoporous films that can be used as a template for colloidal self-assembly. Figure 2 presents the results of such efforts where PS-*b*-PEO BCP and TTIP are used as a structure-directing agent and titanium precursor, respectively. PEO blocks are well-known to form the coordination bond with TTIP, which enables PEO-containing BCP to act as a structure-directing agent in sol−gel process via their self-assembling process. As can be seen in the figure, the final morphologies of calcined titania films are strongly affected by the solution composition and processing conditions. At lower precursor concentrations, tiny spheres of titania are produced to form the films with irregular order, as implied in Figure 2a. However, as the amount of TTIP precursor increases, the structure of the titania films changes from the spheres to the continuous films with nanopores, and the degree of order of the pore array becomes better with further increasing the TTIP precursor, as seen in the Fourier transforms in the insets. Especially, TiO_2 mesoporous films in Figure 2c possess a high degree of lateral order of pores with a pore-to-pore distance of ∼50 nm over a large area, which means that they can be used as a perfect template for colloidal self-assembly of 50-nm PS nanoparticles. (See Figure S2 in the Supporting Information.) Relative humidity (RH) is another important parameter to affect the morphology of calcined films. A highly ordered array of nanopores is produced at higher humidity, while the order of array of nanopores is very poor at lower humidity, as seen in Figures 2c and 2d. Generally, the addition of the precursor solution containing IPA and HCl to the BCP solution in 1,4-dioxane leads to the formation of micelles of PS-*b*-PEO with PEO blocks as a core component, since the water in HCl added to the precursor solution is a poor solvent for PS. Therefore, at lower concentration, all the precursors added to the solution migrate into the core region of micelles, and small-sized titania particles are obtained after the removal of BCP via calcination. However, as the precursor concentration increases, the phase is inverted to form the reverse structure, which leads to the pore structure after calcination. Controlling the processing conditions to be able to affect the reaction rate and the interaction with block components (for example, humidity) results in the formation of a highly ordered array of pores in TiO_2 films that have barely been reported previously, which is one of the great advantages of our approach for templation of colloidal self-assembly. In conclusion, the mesoporous film shown in Figure 2C is employed as a template for guiding the self-assembly of colloidal particles 50 nm in size.

In order to explore the pore structure inside the film in detail, grazing-incidence small-angle scattering (GISAXS) experiments were performed for the films before and after calcination, and the results are presented in Figures 2e and 2f. In both cases, higher-order peaks are observed in the GISAXS patterns and intensity profiles for films presented in Figure 2c to indicate the highly ordered array of the nanostructure and pores with hexagonal packing. After calcination, the peak intensity increases significantly, as seen in the inset of Figure 2f, where the first peak of the profile scanned at the reflection position is saturated and truncated, confirming the pore formation in the film. Furthermore, the strong streaks in the scattering patterns of Figures 2e and 2f indicate that the pores generated via calcination are oriented normal to the surface and span the entire thickness of the films. The distance between neighboring pores is measured from the peak position to be ∼50 nm, which exactly corresponds to the size of PS colloidal particles. These results suggest that our TiO_2 mesoporous film can perfectly act as a template for the self-assembly of 50-nm PS colloidal particles, and, at the same time, the straight pore channels can provide effective pathways with functional materials to access the inside of the template film. This is another great advantage that our approach offers, because our process easily forms hierarchical nanochannels that are connected from the top to bottom surfaces throughout the films when the colloidal crystals fabricated on them are used to produce the inverse opal structure by using the same type of precursors. In the end, this process generates highly porous TiO_2 films with hierarchically ordered pores that are connected from the top to bottom surfaces, which will be shown later.

Attempts to control the self-assembly of colloidal particles by using the template have been reported in the literature, with regard to the crystallization of colloidal particles assisted by the templates. Indeed, template-induced colloidal crystallization has been demonstrated to be a very useful approach to guide the colloidal self-assembly and to create long-range order lattices with few defects.[40−44] However, in most cases, the templates used for the assistance of colloidal assembly have been patterned by top-down approaches such as photolithography, electron-beam lithography, and reactive-ion etching, which means that such an approach has limited access and becomes very expensive and difficult as the feature size decreases. On the other hand, in our approach, the template is generated via the self-assembling process, which is very simple, mass-producible, and easily accessible to everyone. The shape and size of template pattern can be controlled simply by changing the molecular weight and the composition of block components in the case of BCPs.

The effects of mesoporous template on the self-assembly of colloidal particles are demonstrated in Figure 3, where PS

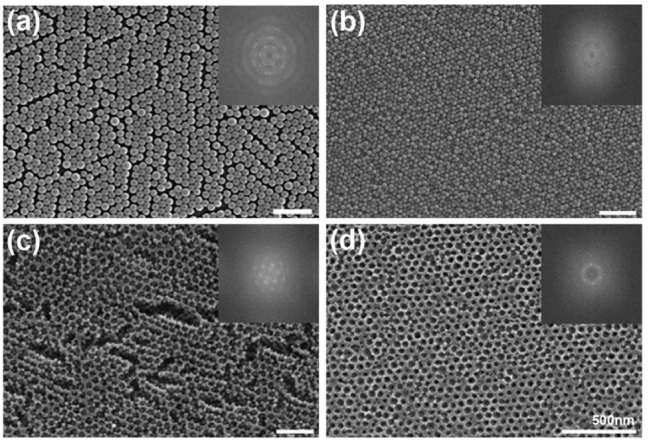

Figure 3. SEM images of (a, b) colloidal crystals and (c, d) their inverse opals fabricated on the template with highly ordered pattern: (a, c) 100-nm and (b, d) 50-nm PS colloidal particles. The insets exhibit the FFT of SEM images.

colloidal particles with diameters of 50 and 100 nm were dip-coated on the mesoporous templates shown in Figure 2c. In the case of 100-nm PS particles that are larger than the characteristic size of the template, the colloidal crystals formed on the template exhibit the same level of degree of order as on the flat substrate without pattern, as shown in Figures 1b and

3a. On the other hand, 50-nm PS particles display the dramatic effects of their template on the colloidal self-assembly, as shown in Figure 3b, where the degree of order of the colloidal crystals is significantly enhanced on the template with highly ordered hexagonal patterns, compared to that on the flat substrate shown in Figure 1c. These results show that a mesoporous pattern can effectively guide the self-assembly of PS nanoparticles with comparable size to generate highly ordered colloidal crystals while the self-assembly of 100-nm PS particles proceeds irrespective of the presence of the template, because of the size mismatch between the colloidal particles and the template pattern. The inverse opal structure on the template exactly reflects that of colloidal crystals, and, as shown in Figure 3d and Figure S3 in the Supporting Information, the inverse opal of 50-nm PS colloidal crystals is truly remarkable, exhibiting a highly ordered porous structure over a large area. Therefore, the final mesoporous TiO_2 film has the two-layer, hybrid structure with the same materials but with different sizes of pores, where the bottom layer has pores 20 nm in size, corresponding to the size of block domains, while its top layer is composed of 50-nm pores, corresponding to the particle size. In terms of the hybrid structure, a similar approach has been reported previously where high-surface mesoporous films with a three-dimensional (3D) colloidal crystal overlayer were fabricated on the porous structure obtained by using a BCP self-assembly to form a double-layered structure with two length scales at the mesoporous and microporous levels.[33] However, in those cases, two self-assemblies of BCPs and colloidal crystals independently proceeded, which means that the colloidal crystals were produced regardless of the structure of mesoporous films underneath them. Those results are very similar to the case in Figure 3c, and as a result, it is highly possible that many pores in the bottom layer would be clogged by the inverse opal film in the top layer, because of the size mismatch. Moreover, the structure of their mesoporous films in the bottom was not so well-controlled as in our case, exhibiting the array of pores with poor order. On the other hand, our hierarchically porous films are based on highly ordered arrays of mesopores that can ultimately guide the self-assembly of colloidal particles, maintaining the high degree of lateral order from the top to bottom layers. In the case of 50-nm colloidal particles, PS particles at the first layer of colloidal crystal sit on the pores at the bottom template, and accordingly, after removal of PS particles, the pores with different length scales span all the way from the top to the bottom of the film without clogging. These features offer great opportunity to fully utilize large TiO_2 surface areas exposed at each pore in many applications, such as photovoltaics and photocatalysts. Furthermore, the pores with large size at the top of the film will easily drive other molecules to get inside pores with smaller size, being able to increase the probability for better performance in applications. This aspect will be revisited in the later part of the paper.

The order of colloidal crystals on the template will be very sensitive to the template size. In our case, the characteristic size of the templates can be controlled by changing the molecular weight of BCP and the relative amount of titanium precursor and BCP solution. The results are presented in Figure 4, where the periodic size of template pattern was varied in the range from 44 nm to 54 nm by slightly increasing the amount of precursor solution in the BCP solution or using different PS-*b*-PEO BCPs. Although all the templates still maintain their highly ordered structures, the 50-nm PS particles show colloidal

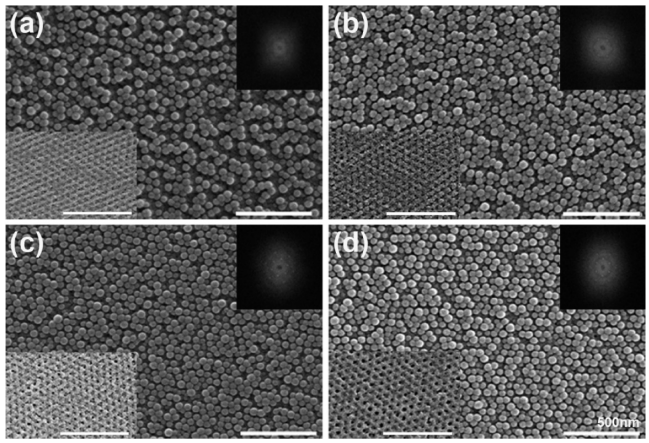

Figure 4. Colloidal crystals of 50-nm PS nanoparticles on template with hexagonal patterns of different characteristic size of (a) 44, (b) 48, (c) 52, and (d) 56 nm. The inset in each figure shows the surface structure of templates used for fabrication of 50-nm PS colloidal crystals.

crystals with significant defects on the template whose characteristic size is less than 50 nm. On the other hand, the templates with pore sizes slightly larger than the particle diameter are shown to be still able to function as a guide to the self-assembly of colloidal particles, as shown in Figures 4c and 4d.

In addition to the variation of the size, the change in the pattern of template will also affect the packing and order of the colloidal crystals. One of the advantages of using BCPs as a structure-directing agent is their ability to generate various morphologies simply by changing the relative amount of BCP and precursor solutions, the processing conditions, or the solvent used for BCP solution. Two additional examples to direct the self-assembly of colloidal particles are illustrated in Figure 5, where the templates have the line pattern and bowl

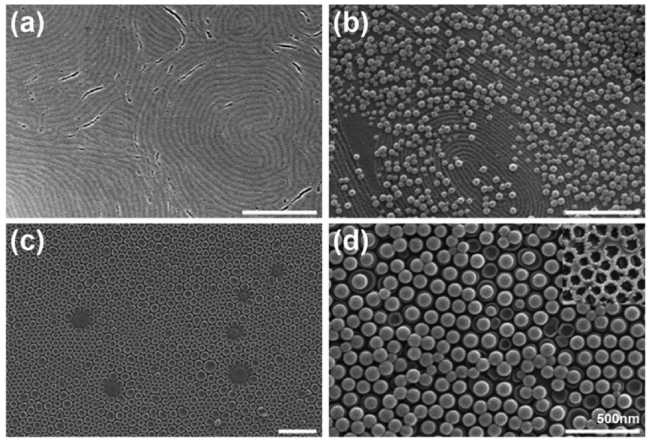

Figure 5. Effect of templates with different patterns on the self-assembly of 50-nm PS colloidal particles: (a, b) line pattern and (c, d) bowl structure.

structure, respectively. The line pattern was produced by changing the relative amount of BCP and precursor solutions, and the bowl pattern was generated by using toluene as a solvent instead of 1,4-dioxane. In both cases, PS colloidal particles are shown to self-assemble along the template pattern whenever their characteristic size matches that of colloidal

particles. Consequently, the particles are located along the line pattern of the template, as shown in Figure 5b, while the PS particles nicely sit inside the bowls via the dip-coating, as seen in Figure 5d. Inversion of bowl structure containing the colloidal particles via infiltration of TiO_2 precursors and calcination produces a very interesting structure after removal of the PS particles, as shown in the inset of Figure 5d. All these results indicate that directed self-assembly of colloidal particles, under the guidance of the template, can produce as many various patterns as the BCPs can. With better understanding and improved techniques for controlling BCP self-assembly, our process can be applied to (i) overcome the limitations resulting from restricted number of their self-assembled patterns and (ii) generate colloidal crystals having a high degree of order with various patterns and sizes.

The mesoporous titania films with two different length scales at the bottom and top layers, especially having the pore connectivity from the top to the bottom without clogging, allow full access to the pore surfaces, which will provide a great opportunity for applications requiring large surface area. Moreover, wider pores at the top can help to funnel the functional materials into smaller-sized pores at the bottom, which enables mesoporous titania films to accommodate a larger size of materials inside the pores, maximizing their performance in applications. In order to explore the potential and efficiency of the hybrid structure in its applications, the photocatalytic ability of mesoporous TiO_2 films with different structures was investigated in this work, and the results are presented in Figure 6. All porous titania films were set to have

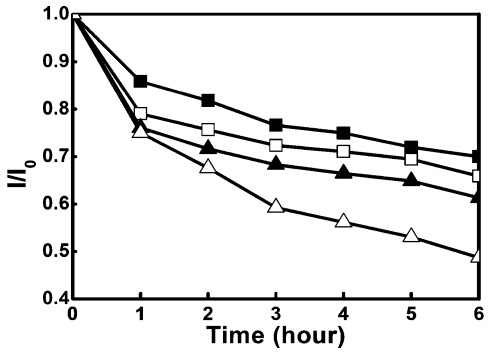

Figure 6. Photocatalytic activity of TiO_2 films with different structures of Methylene Blue (MB) degradation: (■) flat film, (□) mesoporous film based on the self-assembly of BCP, (▲) mesoporous film based on the self-assembly of 50-nm PS nanoparticles, and (△) hierarchically mesoporous film based on the self-assembly of BCP and PS nanoparticles.

the same thickness in order to compare their photocatalytic effects under the same condition. Examination of the catalytic effects of TiO_2 films on the photodegradation of Methylene Blue (MB) reveals that hierarchically mesoporous TiO_2 films that are generated by the dual-templating method based on the self-assembly of BCPs and colloidal particles exhibit much improved photocatalytic effects, as compared with porous TiO_2 films by BCP self-assembly alone or colloidal particles self-assembly alone. Such results indicate that not only our mesoporous TiO_2 films provide large surface area for photodegradation reaction but also wider pores at the top of the films help mass transfer inside narrow pores for better contact. This result is quite interesting, because such hierarchically mesoporous films with a larger size of pores at the top than those at the bottom can be utilized in applications where a small size of hole is required for large surface areas while its small size limits the inclusion and contacts of reactants, for example, the inclusion of poly(3-hexylthiophene) into mesoporous TiO_2 films for the application of photovoltaic cells.[45,46]

■ CONCLUSIONS

In this work, hierarchically ordered mesoporous TiO_2 films, especially possessing a high degree of lateral order, were produced on the sub-100-nm scale by virtue of a new dual-templating method. The first template was prepared via the self-assembly of a block co-polymer (BCP) combined with sol–gel reaction, which produced the TiO_2 films with well-ordered pores on a scale of ∼20 nm. The second one was prepared via the self-assembly of colloidal particles on the first template, which was then used to generate the inverse opal TiO_2 films with well-ordered pores on a scale of ∼50 nm. Our dual-templating approach, which produces hierarchically porous films, provides several advantages over the other previous methods. First, our approach using two templates in sequence is based on the self-assembling behavior, and so the entire process is very simple and requires no expensive machinery to control the final structure. Second, hierarchically porous films fabricated in this work exhibit an exceptionally high degree of lateral order on the sub-100-nm scale. BCP self-assembling behavior can be carefully controlled by optimizing the experimental conditions, and their structure can be tuned by changing the composition and processing parameters. Third, despite the dual-templating approach and the generation of two pores with different sizes, the different types of pores are connected and thus the pores span from the top to the bottom throughout the entire film without clogging, since the second template is prepared by using the first template. Fourth, the pores at the film surface have a wide entrance, which will help other substances get inside the pores and have better contact. These features are very important in applications requiring a large surface area and accessibility for good contact. Normally, it is not easy for substances including macromolecules and electrolytes to access inside holes sub-100 nm in size (in our case, with a diameter of ∼20 nm). However, the large size of holes at the top of the film will give other molecules more chances to get inside into the small-sized holes and keep better contact with the substrate, maximizing the effects of large surface area and producing better performance in applications. In this work, the photocatalytic effect was shown to be enhanced for the porous films with a hierarchical order based on our approach.

Our dual-templating approach, based on the self-assembly of BCP and colloidal particles, offers a very simple yet efficient route to generate hierarchically ordered mesoporous films with a high degree of order. Especially, such porous films with the interconnection of holes and wide entrance will be expected for better contact with functional materials and much-improved performance in various applications that demand the large surface area.

■ ASSOCIATED CONTENT

Supporting Information

SEM images of colloidal crystals fabricated via drop-casting and sedimentation methods; SEM images of the first and second mesoporous layers showing long-range lateral order over a large area. This material is available free of charge via the Internet at http://pubs.acs.org.

AUTHOR INFORMATION

Corresponding Author

*Tel.: +82-32-860-7493. Fax: +82-32-873-0181. E-mail: shk@inha.ac.kr.

Notes

The authors declare no competing financial interest.

ACKNOWLEDGMENTS

This work was financially supported by Basic Science Research Program through the National Research Foundation of Korea (NRF) grant funded by the Korean Government (MEST) (No. 2010-0014451, No. 2012-R1A1A2042942). Experiments at PLS were supported in part by MEST and POSTECH.

REFERENCES

(1) Pan, J. H.; Zhao, X. S.; Lee, W. I. Block Copolymer-templated Synthesis of Highly Organized Mesoporous TiO_2-based Films and Their Photoelectrochemical Applications. *Chem. Eng. J.* **2011**, *170*, 363−380.

(2) Coakley, K. M.; Liu, Y. X.; McGehee, M. D.; Frindell, K. L.; Stucky, G. D. Infiltrating Semiconducting Polymers into Self-assembled Mesoporous Titania Films for Photovoltaic Applications. *Adv. Funct. Mater.* **2003**, *13*, 301−306.

(3) Nedelcu, M.; Guldin, S.; Orilall, M. C.; Lee, J.; Huttner, S.; Crossland, E. J. W.; Warren, S. C.; Ducati, C.; Laity, P. R.; Eder, D.; Wiesner, U.; Steiner, U.; Snaith, H. J. Monolithic Route to Efficient Dye-sensitized Solar Cells Employing Diblock Copolymers for Mesoporous TiO_2. *J. Mater. Chem.* **2010**, *20*, 1261−1268.

(4) Song, Y. Y.; Gao, Z. D.; Wang, J. H.; Xia, X. H.; Lynch, R. Multistage Coloring Electrochromic Device Based on TiO_2 Nanotube Arrays Modified with WO_3 Nanoparticles. *Adv. Funct. Mater.* **2011**, *21*, 1941−1946.

(5) Martinez-Ferrero, E.; Sakatani, Y.; Boissiere, C.; Grosso, D.; Fuertes, A.; Fraxedas, J.; Sanchez, C. Nanostructured Titanium Oxynitride Porous Thin Films as Efficient Visible-Active Photocatalysts. *Adv. Funct. Mater.* **2007**, *17*, 3348−3354.

(6) Wang, X. C.; Yu, J. C.; Ho, C. M.; Hou, Y. D.; Fu, X. Z. Photocatalytic Activity of a Hierarchically Macro/mesoporous Titania. *Langmuir* **2005**, *21*, 2552−2559.

(7) Yu, J. C.; Wang, X. C.; Fu, X. Z. Pore-wall Chemistry and Photocatalytic Activity of Mesoporous Titania Molecular Sieve Films. *Chem. Mater.* **2004**, *16*, 1523−1530.

(8) Frindell, K. L.; Bartl, M. H.; Robinson, M. R.; Bazan, G. C.; Popitsch, A.; Stucky, G. D. Visible and Near-IR Luminescence via Energy Transfer in Rare Earth Doped Mesoporous Titania Thin Films with Nanocrystalline Walls. *J. Solid State Chem.* **2003**, *172*, 81−88.

(9) Liu, G.; Chen, Z. G.; Dong, C. L.; Zhao, Y. N.; Li, F.; Lu, G. Q.; Cheng, H. M. Visible Light Photocatalyst: Iodine-doped Mesoporous Titania with a Bicrystalline Framework. *J. Phys. Chem. B* **2006**, *110*, 20823−20828.

(10) Fu, X. N.; Liu, J.; Yang, H.; Sun, J. C.; Li, X.; Zhang, X. K.; Jia, Y. X. Arrays of Au-TiO_2 Janus-like Nanoparticles Fabricated by Block Copolymer Templates and Their Photocatalytic Activity in the Degradation of Methylene Blue. *Mater. Chem. Phys.* **2011**, *130*, 334−339.

(11) Lin, K. H.; Crocker, J. C.; Prasad, V.; Schofield, A.; Weitz, D. A.; Lubensky, T. C.; Yodh, A. G. Entropically Driven Colloidal Crystallization on Patterned Surfaces. *Phys. Rev. Lett.* **2000**, *85*, 1770−1773.

(12) Kaune, G.; Memesa, M.; Meier, R.; Ruderer, M. A.; Diethert, A.; Roth, S. V.; D'Acunzi, M.; Gutmann, J. S.; Muller-Buschbaum, P. Hierarchically Structured Titania Films Prepared by Polymer/Colloidal Templating. *ACS Appl. Mater. Interfaces* **2009**, *1*, 2862−2869.

(13) Dziomkina, N. V.; Hempenius, M. A.; Vancso, G. J. Symmetry Control of Polymer Colloidal Monolayers and Crystals by Electrophoretic Deposition onto Patterned Surfaces. *Adv. Mater.* **2005**, *17*, 237−240.

(14) Qi, L.; Birnie, D. P. Templated Titania Films with Meso- and Macroporosities. *Mater. Lett.* **2007**, *61*, 2191−2194.

(15) Deng, Y. H.; Liu, C.; Yu, T.; Liu, F.; Zhang, F. Q.; Wan, Y.; Zhang, L. J.; Wang, C. C.; Tu, B.; Webley, P. A.; Wang, H. T.; Zhao, D. Y. Facile Synthesis of Hierarchically Porous Carbons from Dual Colloidal Crystal/Block Copolymer Template Approach. *Chem. Mater.* **2007**, *19*, 3271−3277.

(16) Wu, C. W.; Ohsuna, T.; Kuwabara, M.; Kuroda, K. Formation of Highly Ordered Mesoporous Titania Films Consisting of Crystalline Nanopillars with Inverse Mesospace by Structural Transformation. *J. Am. Chem. Soc.* **2006**, *128*, 4544−4545.

(17) Cheng, Y. J.; Zhou, S. Y.; Gutmann, J. S. Morphology Transition in Ultrathin Titania Films: From Pores to Lamellae. *Macromol. Rapid Commun.* **2007**, *28*, 1392−1396.

(18) Feng, D.; Luo, W.; Zhang, J. Y.; Xu, M.; Zhang, R. Y.; Wu, H. Y.; Lv, Y. Y.; Asiri, A. M.; Khan, S. B.; Rahman, M. M.; Zheng, G. F.; Zhao, D. Y. Multi-layered Mesoporous TiO_2 Thin Films with Large Pores and Highly Crystalline Frameworks for Efficient Photoelectrochemical Conversion. *J. Mater. Chem. A* **2013**, *1*, 1591−1599.

(19) Meng, X. J.; Kimura, T.; Ohji, T.; Kato, K. Triblock Copolymer Templated Semi-crystalline Mesoporous Titania Films Containing Emulsion-Induced Macropores. *J. Mater. Chem.* **2009**, *19*, 1894−1900.

(20) Chandra, D.; Ohji, T.; Kato, K.; Kimura, T. Connectivity of PS-b-PEO Templated Spherical Pores in Titanium Oxide Films. *Phys. Chem. Chem. Phys.* **2011**, *13*, 12529−12535.

(21) Gutierrez, J.; Tercjak, A.; Garcia, I.; Peponi, L.; Mondragon, I. Hybrid Titanium Dioxide/PS-b-PEO Block Copolymer Nanocomposites Based on Sol-gel Synthesis. *Nanotechnology* **2008**, *19*, 155607−155614.

(22) Cheng, Y. J.; Gutmann, J. S. Morphology Phase Diagram of Ultrathin Anatase TiO_2 Films Templated by a Single PS-b-PEO block Copolymer. *J. Am. Chem. Soc.* **2006**, *128*, 4658−4674.

(23) Li, X.; Peng, J.; Kang, J. H.; Choy, J. H.; Steinhart, M.; Knoll, W.; Kim, D. H. One Step Route to the Fabrication of Arrays of TiO_2 Nanobowls via a Complementary Block Copolymer Templating and Sol−Gel Process. *Soft Matter* **2008**, *4*, 515−521.

(24) Scalarone, D.; Tata, J.; Caldera, F.; Lazzari, M.; Chiantore, O. Porous and Worm-like Titanium Dioxide Nanostructures from PS-b-PEO Block Copolymer Micellar Solutions. *Mater. Chem. Phys.* **2011**, *128*, 166−171.

(25) Zhao, J. Q.; Wan, P.; Xiang, J.; Tong, T.; Dong, L.; Gao, Z. N.; Shen, X. Y.; Tong, H. Synthesis of Highly Ordered Macro-mesoporous Anatase TiO_2 Film with High Photocatalytic Activity. *Microporous Mesoporous Mater.* **2011**, *138*, 200−206.

(26) Docampo, P.; Stefik, M.; Guldin, S.; Gunning, R.; Yufa, N. A.; Cai, N.; Wang, P.; Steiner, U.; Wiesner, U.; Snaith, H. J. Triblock-Terpolymer-Directed Self-Assembly of Mesoporous TiO_2: High-Performance Photoanodes for Solid-State Dye-Sensitized Solar Cells. *Adv. Energy Mater.* **2012**, *2*, 676−682.

(27) Dionigi, C.; Greco, P.; Ruani, G.; Cavallini, M.; Borgatti, F.; Biscarini, F. 3D Hierarchical Porous TiO_2 Films from Colloidal Composite Fluidic Deposition. *Chem. Mater.* **2008**, *20*, 7130−7135.

(28) Jia, L. C.; Cai, W. P.; Wang, H. Q.; Sun, F. Q.; Li, Y. Hetero-apertured Micro/Nanostructured Ordered Porous Array: Layer-by-Layered Construction and Structure-Induced Sensing Parameter Controllability. *ACS Nano* **2009**, *3*, 2697−2705.

(29) Iskandar, F.; Iwaki, T.; Toda, T.; Okuyama, K. High Coercivity of Ordered Macroporous FePt Films Synthesized via Colloidal Templates. *Nano Lett.* **2005**, *5*, 1525−1528.

(30) Kuo, C. W.; Shiu, J. Y.; Wei, K. H.; Chen, P. Monolithic Integration of Well-ordered Nanoporous Structures in the Microfluidic Channels for Bioseparation. *J. Chromatogr. A* **2007**, *1162*, 175−179.

(31) Henrist, C.; Dewalque, J.; Cloots, R.; Vertruyen, B.; Jonlet, J.; Colson, P. Hierarchical Porous TiO_2 Thin Films by Soft and Dual Templating: A Quantitative Approach of Specific Surface and Porosity. *Thin Solid Films* **2013**, *539*, 188−193.

(32) Liu, J.; Li, M. Z.; Wang, J. X.; Song, Y. L.; Jiang, L.; Murakami, T.; Fujishima, A. Hierarchically Macro-/Mesoporous Ti-Si Oxides

Photonic Crystal with Highly Efficient Photocatalytic Capability. *Environ. Sci. Technol.* **2009**, *43*, 9425−9431.
(33) Guldin, S.; Huttner, S.; Kolle, M.; Welland, M. E.; Muller-Buschbaum, P.; Friend, R. H.; Steiner, U.; Tetreault, N. Dye-Sensitized Solar Cell Based on a Three-Dimensional Photonic Crystal. *Nano Lett.* **2010**, *10*, 2303−2309.
(34) Ramiro-Manzano, F.; Bonet, E.; Rodriguez, I.; Meseguer, F. Colloidal Crystal Thin Films Grown into Corrugated Surface Templates. *Langmuir* **2010**, *26*, 4559−4562.
(35) Hur, J.; Won, Y. Y. Fabrication of High-quality Non-close-packed 2D Colloid Crystals by Template-Guided Langmuir−Blodgett Particle Deposition. *Soft Matter* **2008**, *4*, 1261−1269.
(36) Juillerat, F.; Solak, H. H.; Bowen, P.; Hofmann, H. Fabrication of Large-area Ordered Arrays of Nanoparticles on Patterned Substrates. *Nanotechnology* **2005**, *16*, 1311−1316.
(37) Bae, C.; Shin, H.; Moon, J. Facile Route to Aligned One-Dimensional Arrays of Colloidal Nanoparticles. *Chem. Mater.* **2007**, *19*, 1531−1533.
(38) Hyun, D. C.; Moon, G. D.; Cho, E. C.; Jeong, U. Y. Repeated Transfer of Colloidal Patterns by Using Reversible Buckling Process. *Adv. Funct. Mater.* **2009**, *19*, 2155−2162.
(39) Hoogenboom, J. P.; Retif, C.; de Bres, E.; de Boer, M. V.; van Langen-Suurling, A. K.; Romijn, J.; van Blaaderen, A. Template-induced Growth of Close-Packed and Non-close-packed Colloidal Crystals During Solvent Evaporation. *Nano Lett.* **2004**, *4*, 205−208.
(40) Ye, R.; Ye, Y. H.; Zhou, Z. T.; Xu, H. H. Gravity-Assisted Convective Assembly of Centimeter-Sized Uniform Two-Dimensional Colloidal Crystals. *Langmuir* **2013**, *29*, 1796−1801.
(41) Bardosova, M.; Pemble, M. E.; Povey, I. M.; Tredgold, R. H. The Langmuir−Blodgett Approach to Making Colloidal Photonic Crystals from Silica Spheres. *Adv. Mater.* **2010**, *22*, 3104−3124.
(42) Meijer, J. M.; Hagemans, F.; Rossi, L.; Byelov, D. V.; Castillo, S. I. R.; Snigirev, A.; Snigireva, I.; Philipse, A. P.; Petukhov, A. V. Self-Assembly of Colloidal Cubes via Vertical Deposition. *Langmuir* **2012**, *28*, 7631−7638.
(43) Fu, Y. N.; Jin, Z. G.; Liu, G. Q.; Yin, Y. X. Self-assembly of Polystyrene Sphere Colloidal Crystals by In Situ Solvent Evaporation Method. *Synth. Met.* **2009**, *159*, 1744−1750.
(44) Njoya, N. K.; Birdsall, R. E.; Wirth, M. J. Silica Colloidal Crystals as Emerging Materials for High-Throughput Protein Electrophoresis. *AAPS J.* **2013**, *15*, 962−969.
(45) Rawolle, M.; Sarkar, K.; Niedermeier, M. A.; Schindler, M.; Lellig, P.; Gutmann, J. S.; Moulin, J. F.; Haese-Seiller, M.; Wochnik, A. S.; Scheu, C.; Muller-Buschbaum, P. Infiltration of Polymer Hole−Conductor into Mesoporous Titania Structures for Solid-State Dye-Sensitized Solar Cells. *ACS Appl. Mater. Interfaces* **2013**, *5*, 719−729.
(46) Kaune, G.; Haese-Seiller, M.; Kampmann, R.; Moulin, J. F.; Zhong, G.; Muller-Buschbaum, P. TOF-GISANS Investigation of Polymer Infiltration in Mesoporous TiO_2 Films for Photovoltaic Applications. *J. Polym. Sci., Part B: Polym. Phys.* **2010**, *48*, 1628−1635.